

Confident Detection of Doubly-Ionized Thorium in the Extreme Ap Star CPD-62° 2717

S. Drew Chojnowski^{1, *}, Svetlana Hubrig², David L. Nidever¹, Ewa Niemczura³, Jonathan Labadie-Bartz⁴, Gautier Mathys⁵, Sten Hasselquist⁶

¹*Department of Physics, Montana State University, P.O. Box 173840, Bozeman, MT 59717-3840*

²*Leibniz-Institut für Astrophysik Potsdam (AIP), An der Sternwarte 16, 14482 Potsdam, Germany*

³*Instytut Astronomiczny, Uniwersytet Wrocławski, Kopernika 11, 51-622 Wrocław, Poland*

⁴*LESIA, Paris Observatory, PSL University, CNRS, Sorbonne Université, Université de Paris, 5 place Jules Janssen, 92195 Meudon, France*

⁵*European Southern Observatory, Alonso de Cordova 3107, Vitacura, Santiago, Chile*

⁶*Space Telescope Science Institute, 3700 San Martin Drive, Baltimore, MD 21218, USA*

Accepted XXX. Received YYY; in original form ZZZ

ABSTRACT

Despite the universe containing primordial thorium (Th) of sufficient abundance to appear in stellar spectra, detection of Th has to date been tentative and based on just a few weak and blended lines. Here, we present convincing evidence not only for the first Th detection in a magnetic chemically peculiar Ap star but also for the first detection of Th III in a stellar spectrum. CPD-62° 2717 was initially recognized as a highly-magnetized Ap star thanks to resolved magnetically split lines captured in *H*-band spectra from the SDSS/APOGEE survey. The star was subsequently pinpointed as extraordinarily peculiar when careful inspection of the *H*-band line content revealed the presence of five lines of Th III, none of which are detected in the other ~ 1500 APOGEE-observed Ap stars. Follow-up with the VLT+UVES confirmed a similarly peculiar optical spectrum featuring dozens of Th III lines, among other peculiarities. Unlike past claims of Th detection, and owing to high-resolution observations of the strong (~8–12 kG) magnetic field of CPD-62° 2717, the detection of Th III can in this case be supported by matches between the observed and theoretical magnetic splitting patterns. Comparison of CPD-62° 2717 to stars for which Th overabundances have been previously reported (e.g., Przybylski’s Star) indicate that only for CPD-62° 2717 is the Th detection certain. Along with the focus on Th III, we use time series measurements of the magnetic field modulus to constrain the rotation period of CPD-62° 2717 to ~4.8 years, thus establishing it as a new example of a super-slowly-rotating Ap star.

Key words: stars: magnetic fields – stars: chemically peculiar

1 INTRODUCTION

Considering the unknown origin of super-strong magnetic fields in stars that are expected to have mostly if not fully radiative envelopes, there is no such thing as a ‘normal’ Ap star. However, since being defined more than 60 years ago (Babcock 1958) as a distinct sub-group of slowly rotating, highly magnetized, mostly A-type stars whose spectra show chemical peculiarities when compared to their non-magnetic analogues, a few examples have stood out as particularly peculiar and extreme. Perhaps the best-known and most peculiar Ap star (if not the most peculiar star in general) is HD 101065, also known as Przybylski’s Star. It was named after its discoverer (Przybylski 1961), and will be referred to as “PS” throughout this work.

In his initial studies of optical spectra of PS, Przybylski struggled to identify any light elements aside from hydrogen and calcium, instead finding only a few lines of strontium and barium and literally thousands of lines from rare earth elements (or REE; $57 \leq Z \leq 71$; Przybylski & Kennedy 1963). Even though the vast majority of Ap stars exhibit surface underabundances of light elements like helium

and often extreme overabundances of heavier elements, the fact that elements like iron seemed to be missing altogether from spectra of PS left astronomers baffled for years (Przybylski 1977). Lines from gold have yet to be confidently identified in spectra of PS and might never be owing to the pileup of strong lines from singly-ionized REE around the wavelengths of the known optical Au II lines, but PS can nonetheless be considered a spectroscopic goldmine. Remarkably, the presence of the REE holmium was confirmed in the atmosphere of PS before it had been confirmed in any other star including the Sun (Przybylski 1963).

Whereas the surface abundances of PS are undoubtedly extreme, the associated 2.3 kG global magnetic field (Wolff & Hagen 1976; Cowley et al. 2000) of PS is certainly not given that Ap star magnetic fields can reach extraordinary strengths of up to 34 kG (in the case of Babcock’s Star; Babcock 1960), with numerous examples of >10 kG (Mathys 2017; Giarrusso et al. 2022; Chojnowski et al. 2019). On the other hand, the effective temperature of PS ($T_{\text{eff}} \approx 6500$ K, hence Fp being more accurate than Ap; Cowley et al. 2000; Shulyak et al. 2010) places it at the extreme cool end of the known T_{eff} range for Ap stars and the possible 188 year rotation period (Hubrig et al. 2018) places PS as the most extreme member of the super-slowly

* E-mail: stephen.chojnowski@montana.edu

rotating Ap stars (ssrAp; Mathys et al. 2022). In addition to the spectroscopic peculiarities, PS is photometrically variable due to non-radial pulsation with a ~ 12 minute period (Kurtz & Wegner 1979). PS was the first known example of what are now referred to as rapidly oscillating Ap stars (or roAp; Kurtz 1982).

Motivated by knowledge of the long-lived isotopes of the mostly radioactive actinides thorium (half-life of ≈ 14 Gyr for ^{232}Th) and uranium (half-life of ≈ 4.5 Gyr for ^{238}U) that are formed purely by r -process events, claims of the presence of these elements in the atmosphere of PS date back to as early as Cowley et al. (1977). Of the shockingly few (~ 200) Ap stars for which chemical abundances have been reported in the literature (Ghazaryan et al. 2018), PS leads the pack in terms of $[\text{Th}/\text{H}]$ (enhanced by between 2.75–3.89 dex relative to solar; Cowley et al. 2000; Shulyak et al. 2010). Similarly, the claimed $[\text{U}/\text{H}]$ enhancement (between 2.82–4.12 over solar; Cowley et al. 2000; Shulyak et al. 2010) is topped only by the upper limit of $[\text{U}/\text{H}] < 4.88$ that was reported without much ado for HD 26385 (Bolcal et al. 1991). The solar Th abundance itself is well constrained by meteoric estimates, but attempts to measure it from the Sun’s photosphere rely on just one line (Th II 4019 Å; e.g., Caffau et al. 2008) that is blended with several other far stronger lines.

The relatively warm ($T_{\text{eff}} = 11\,000$ K; Nielsen et al. 2020) and super-slowly rotating ($P_{\text{rot}} \approx 21.8$ years; Rice 1988) Ap star HR 465 has often been discussed in the context of PS due to similarities such as the strong enhancement of heavy REE (Tb, Dy, Ho, Er) that are absent from the majority of Ap star spectra (e.g., Aikman et al. 1979; Cowley & Greenberg 1987). In fact, HR 465 represents the first literature mentions of Th and U detections in an Ap star spectrum. The claim of a U overabundance came first, with Cowley & Hartoog (1972) reporting that the strengths of three observed features attributed to U II indicated a surface abundance roughly one million times that of the Sun. The Th overabundance claim came subsequently when Cowley et al. (1975) attributed a feature at 4019 Å in the spectrum of HR 465 to Th II, with the line strength indicating a large overabundance, similar to U.

A more recent study by Nielsen et al. (2020) was unable to confirm the presence of Th and U in a modern spectrum of HR 465 taken at a rotation phase of $\phi_{\text{rot}} = 0.68$. The Th II lines seemed to be absent altogether, and while the wavelengths of two unknown features closely corresponded to positions of U II lines, the authors stated that “other stronger transitions from lower energy states do not support the presence of uranium in the stellar photosphere.” Considering the highly variable abundances of HR 465 as a function of rotation phase, including a distinct “REE maximum” phase (Rice 1988) that occurs around $\phi_{\text{rot}} = 0$, it is possible that Th and U were simply weak in the $\phi_{\text{rot}} = 0.68$ spectrum of Nielsen et al. (2020).

Searches for PS and HR 465 analogues (e.g. Hubrig et al. 2002) have turned up a few additional stars – HD 217522 and HD 965 – that share the peculiarity of an overwhelming REE spectrum and that have effective temperatures closer to that of PS (6750 K for HD 217522 and 7500 K for HD 965; Ghazaryan et al. 2018). HD 965 in particular has been involved in the recent PS lore due to claims of detection of promethium (e.g., Aller & Cowley 1970; Cowley et al. 2004; Fivet et al. 2007), which is the only REE without any long-lived isotopes and hence the only REE that should not be present in a stellar atmosphere. Similar to PS, HD 965 is a ssrAp star with a recently determined 16.5-year rotation period (Mathys et al. 2019) and with a relatively modest magnetic field strength of ~ 4.3 kG (Mathys et al. 1997; Giarrusso et al. 2022).

Two common themes among the reports of Th and U detections in Ap star spectra have been a reliance on wavelength coincidence statistics based on unresolved magnetically split lines and a lack of

visual evidence provided (e.g., a plot showing numerous Th and U lines at the expected wavelengths and relative strengths). The best evidence to date of Th and U in stellar atmospheres has actually been provided by a handful of extremely metal-poor, r -process-enhanced Galactic halo stars, the most studied of which is probably CS 31082-001 (Cayrel et al. 2001; Hill et al. 2002). The presence of Th has been shown to be fairly unambiguous for this star, with several Th II lines detected in blue/UV spectra, but the U detection relies on careful treatment of a small dent in the wing of a strong Fe I line that can be attributed to U II. The Th and U abundances of these stars have been used to estimate stellar ages based on comparison to models of the Th and U production ratios in r -process events (e.g. Schatz et al. 2002).

Here, we use a combination of relatively high-resolution near-infrared (NIR) H -band spectra from the Apache Point Observatory Galactic Evolution Experiment (APOGEE; Majewski et al. 2017) and high-resolution optical spectra from the 8.2m Very Large Telescope (VLT) and its UV-Visual Echelle Spectrograph (UVES; Dekker et al. 2000) to establish by far the most convincing detection to date of thorium, and of an actinide in general, in an Ap star atmosphere. The presence of Th III at high abundance on the surface of the Ap star CPD-62° 2717 is supported in both the NIR and optical data not only by matches between observed local minima and known Th III wavelengths but also by matches between the observed Zeeman splitting patterns and those predicted from the atomic data. This Zeeman coincidence statistics (ZCS) method was first suggested as a line identification tool by Mathys & Lanz (1995), and it has been used previously to confirm the detection of neutral lithium in the spectra of cool Ap stars (Kochukhov 2008) as well as to vet the Nd III linelist (Ryabchikova et al. 2006).

Little was known about CPD-62° 2717 prior to the discovery of resolved, magnetically split lines (RMSL) in H -band spectra (Chojnowski et al. 2019) that indicated a mean magnetic field modulus around $\langle B \rangle \sim 8$ kG. The B8 temperature class reported by Loden et al. (1976) seems to be an error given that the 3rd data release of the Gaia mission (DR3; Gaia Collaboration et al. 2016, 2022) indicates a far cooler $T_{\text{eff}} = 6834$ K. Gaia DR3 also quotes a distance of 473 pc, a logarithmic surface gravity of $\log g = 3.92$, a stellar mass of $1.64 M_{\odot}$, and a stellar radius of $2.41 R_{\odot}$, all of which put CPD-62° 2717 in the parameter ballpark of PS (albeit with CPD-62° 2717 being more distant and thus fainter at $V \sim 10.4$). CPD-62° 2717 has also been noted as a photometric variable, with for example the All-Sky Automated Survey for Supernovae (ASAS-SN; Jayasinghe et al. 2018) quoting a 518 d period with an amplitude of 0.2 mag. As will be seen, the rotation period implied by the multi-epoch spectra is considerably longer.

The paper is laid out as follows. Section 2 provides a summary of the data used, while the associated analyses (including the use of time series mean magnetic field modulus measurements for constraining the rotation period of CPD-62° 2717) are detailed in Section 3. Sections 4 and 5 focus on the H -band spectra, providing line identifications as well as evidence of H -band Th III lines. Sections 6 and 7 are similar, but focusing on the optical spectra and solidifying without a doubt the Th III detection. The paper concludes in Section 8 with a discussion of additional stars whose archival UVES spectra show some evidence of Th III.

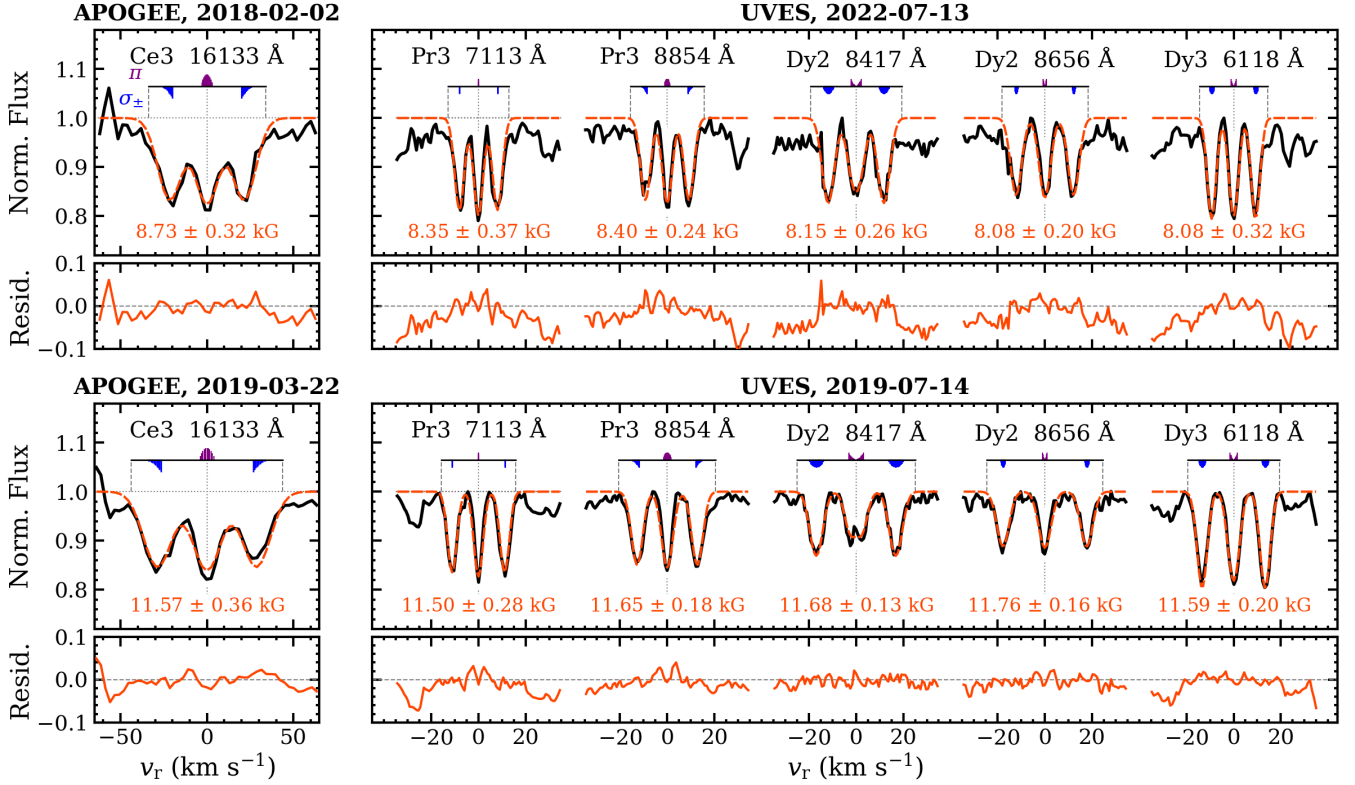


Figure 1. Examples of Gaussian fits to the Ce III 16133 Å line in two APOGEE spectra and to Pr III, Dy II, and Dy III lines in two UVES spectra. Observed minus fit residuals are shown in the smaller panels. In the larger line profile panels, the individual π (upward ticks) and σ_{\pm} (downward ticks) Zeeman components are displayed above each line profile with the fixed relative intensities scaled arbitrarily and with the fixed relative velocity separations scaled to the $\langle B \rangle$ obtained from the fit and quoted below each line profile. Vertical and horizontal dotted lines indicate line centers and continuum level, and vertical dashed lines demonstrate how the windows for direct summation equivalent widths are established on a line-by-line and $\langle B \rangle$ -by- $\langle B \rangle$ basis.

2 SPECTROSCOPIC DATA

2.1 APOGEE *H*-band Spectroscopy

APOGEE is a component of the Sloan Digital Sky Survey (SDSS; e.g., Ahumada et al. 2020) that has been operating on the Sloan 2.5-m telescope (Gunn et al. 2006) at Apache Point Observatory (APO, APOGEE-N) since 2011, and on the Irénée du Pont 2.5-m telescope at Las Campanas Observatory (LCO, APOGEE-S) since 2017. The APOGEE instruments are duplicate 300-fiber, $R \approx 22\,500$ spectrographs (Wilson et al. 2019) that record most of the *H*-band (15145–16960 Å; vacuum wavelengths used throughout this paper when referring to the *H*-band) onto three detectors, with gaps between 15800–15860 Å and 16430–16480 Å due to non-overlapping wavelength coverage of the detectors. For a details of the APOGEE data reduction pipeline, see Nidever et al. (2015), and for details of the APOGEE targeting strategy, see Zasowski et al. (2013).

CPD-62° 2717 was observed by the APOGEE-S instrument a total of 23 times between 2018 February 2 and 2019 March 22, with six distinct groupings of observations separated by one or several days. A 24th observation took place on 2023 April 27, just hours before we received the referee report on this paper. We decided to include this spectrum in the revised manuscript since the associated magnetic field strength estimate helps to constrain our estimate of the rotation period (see Section 3.2).

2.2 VLT/UVES Optical Spectroscopy

CPD-62° 2717 was observed by the UV-visual echelle spectrograph (UVES; Dekker et al. 2000) on the 8.2-m Kueyen unit of the Very Large Telescope (VLT) at the Cerro Paranal Observatory a total of eight times between 2019 April 4 and 2022 August 3. UVES uses a beam splitter to record the most of the optical wavelength range onto two CCDs, achieving resolutions of $R \approx 74\,000$ in the blue when using a 0'4 slit and $R \approx 107\,000$ in the red when using a 0'3 slit. We used a setup that resulted in the blue detector covering 3755–4980 Å and the red detector covering 5688–9459 Å. The data were reduced using version 6.1.3 of the European Southern Observatory (ESO) Reflex software. The UVES observations of CPD-62° 2717 are summarized in Table 1. Due to extreme blending in the UVES blue coverage for CPD-62° 2717, our analyses focus on the red coverage where contributions from iron peak elements and singly-ionized REE (REE2 from here on) are far fewer.

2.3 Linelist

The optical and *H*-band rest wavelengths, oscillator strengths ($\log g f$), and effective Landé factors (g_{eff}) used here were taken primarily from the Vienna Atomic Line Database (VALD; Pakhomov et al. 2019). Although VALD contains lines for most of the doubly-ionized REE (REE3 from here on), ions like Sm III and Gd III are glaring exceptions that likely account for a non-negligible fraction of the plethora of unidentified lines produced by CPD-62° 2717.

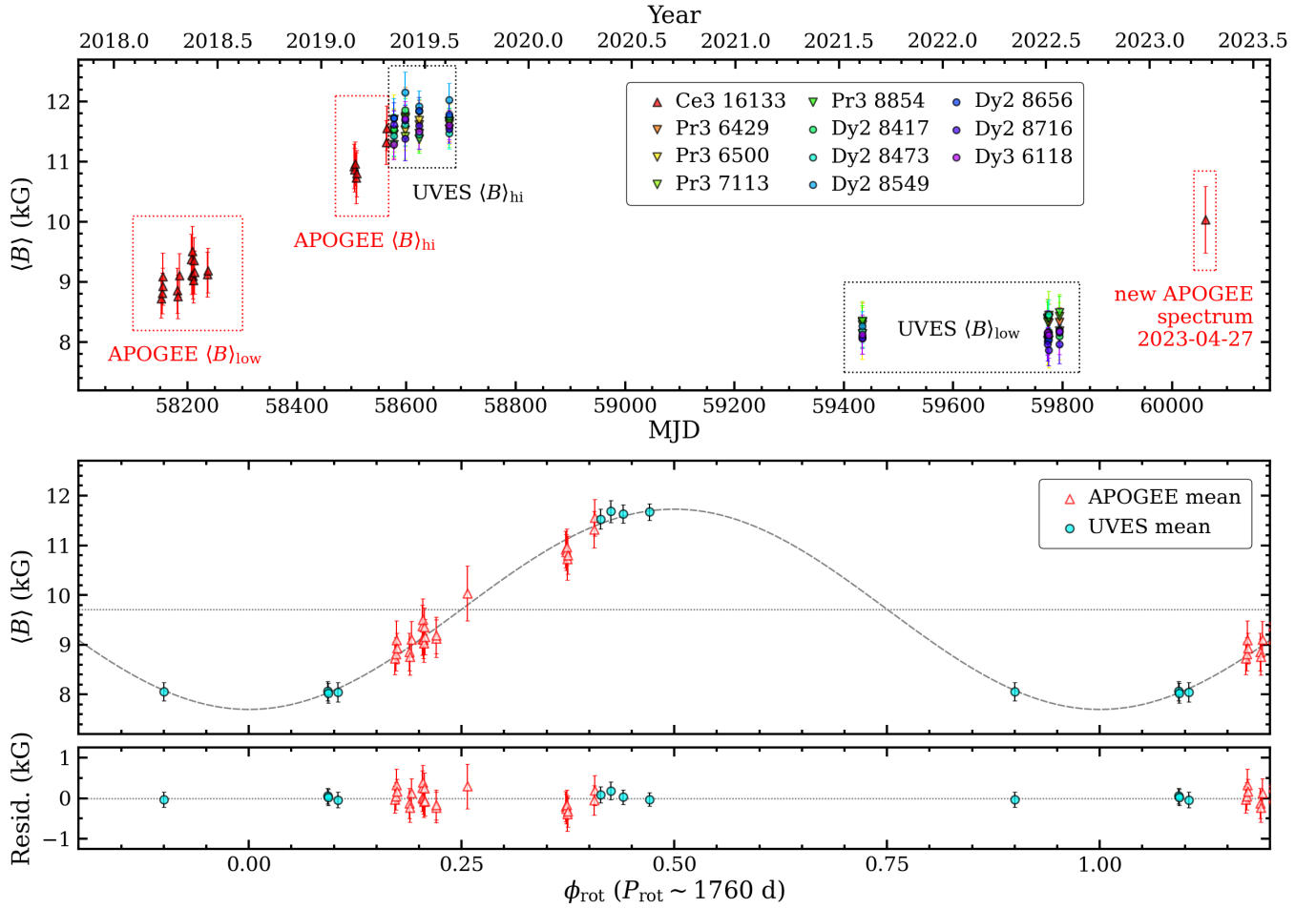


Figure 2. *Upper panel:* the line-by-line $\langle B \rangle$ measurements of CPD-62° 2717 as a function of time. With the exception of the recent APOGEE observation at far right (excluded due to relatively low S/N and intermediate $\langle B \rangle$), the dotted line boxes demonstrate epoch groupings from which the associated spectra were combined. These $\langle B \rangle_{\text{low}}$ and $\langle B \rangle_{\text{hi}}$ spectra will be used for the remainder of this paper. *Lower panels:* the epoch-averaged $\langle B \rangle$ measurements of CPD-62° 2717 phased by a possible 1760 day rotation period, with the dashed curve in the larger panel representing the sine curve that best fits the measurements. Observed minus fit residuals are shown in the smaller panel.

Another exception is Ho II, which is strong for CPD-62° 2717 and for which the National Institute of Standards and Technology (NIST; Kramida et al. 2021) atomic database lists far more lines (albeit lacking most of the important atomic data) than does VALD. U III is another unfortunate omission, since it may also be responsible for some fraction of the unidentified lines and since its detection might allow for a radioactive cosmochronological age estimate for CPD-62° 2717.

Given that this paper presents the first unambiguously demonstrated proof of Th III lines in a stellar spectrum, it does not suffice to simply credit VALD. The optical portion of the Th III linelist was determined experimentally by Biémont et al. (2002), and these authors correctly hypothesized that some Th III lines should appear in the spectra of Ap stars with large overabundances of REE3. The thorium linelist was later extended into the infrared by Redman et al. (2014), with seven of the Th III transitions falling in APOGEE’s coverage of the *H*-band.

3 ANALYSIS

3.1 Magnetic Field Measurement

The spectra of CPD-62° 2717 were analyzed with a Python code (to be made publicly available pending some improvements and full documentation) that performs least-squares fitting of the observed line profiles of one or more atomic transitions with radial velocity (v_r), mean magnetic field modulus ($\langle B \rangle$), full width at half maximum (FWHM), and equivalent width (W_λ) as the variables to be either fixed or allowed to vary. The individual π and σ_\pm Zeeman components of each transition, as determined based on the total angular momentum quantum numbers (J ; which dictate the number of components and their relative strengths) and Landé factors (g ; which dictate the magnitude of the splitting) of the upper and lower energy levels, are approximated as Gaussians of uniform FWHM. The relative strengths and separations of the Zeeman components are fixed to those predicted by the atomic data but scaled in wavelength or velocity space in order to match the observed line profile and thus estimate $\langle B \rangle$.

Once a best fit has been achieved, $\langle B \rangle$ is calculated via $\langle B \rangle = \Delta\lambda \lambda_0^{-2} k^{-1} g_{\text{eff}}^{-1}$, where λ_0 is the rest wavelength of the transition,

Table 1. Summary of spectroscopic observations of CPD-62° 2717. The approximate rotation phases (ϕ_{rot}) were calculated based on the measurements of the mean magnetic field modulus ($\langle B \rangle$). Under the assumption of sinusoidal $\langle B \rangle$ variation, the measurements can be satisfactorily fit using a rotation period of $P_{\text{rot}} = 1760.4$ days and a modified julian data of MJD=57849.9 as an epoch of minimum magnetic field strength.

Date	MJD-Mid	Instrument	t_{exp} (s)	S/N	v_r (km s $^{-1}$)	$\langle B \rangle$ (kG)	ϕ_{rot}
2018-02-02	58151.394	APOGEE-S	501	85	-1.84 ± 0.83	8.73 ± 0.33	0.17
2018-02-04	58153.380	APOGEE-S	2002	177	-2.02 ± 0.83	8.81 ± 0.34	0.17
2018-02-05	58154.336	APOGEE-S	1502	103	-1.93 ± 1.05	9.09 ± 0.40	0.17
2018-02-06	58155.289	APOGEE-S	1001	90	-2.29 ± 0.76	8.93 ± 0.31	0.17
2018-03-04	58181.284	APOGEE-S	2002	165	-2.19 ± 0.98	8.86 ± 0.38	0.19
2018-03-05	58182.289	APOGEE-S	1502	160	-1.74 ± 0.94	8.76 ± 0.36	0.19
2018-03-08	58185.235	APOGEE-S	2503	202	-1.86 ± 0.93	9.11 ± 0.36	0.19
2018-03-30	58207.179	APOGEE-S	2002	167	-2.53 ± 1.18	9.38 ± 0.42	0.20
2018-03-31	58208.193	APOGEE-S	2002	174	-1.31 ± 0.81	9.12 ± 0.32	0.20
2018-04-01	58209.124	APOGEE-S	2002	180	-2.44 ± 1.21	9.51 ± 0.42	0.20
2018-04-02	58210.105	APOGEE-S	2002	148	-2.16 ± 1.00	9.10 ± 0.38	0.21
2018-04-03	58211.165	APOGEE-S	2503	169	-1.94 ± 1.00	9.03 ± 0.38	0.21
2018-04-04	58212.110	APOGEE-S	2002	170	-2.00 ± 1.02	9.36 ± 0.38	0.21
2018-04-05	58213.170	APOGEE-S	2002	170	-1.85 ± 0.94	9.16 ± 0.36	0.21
2018-04-28	58236.094	APOGEE-S	1502	123	-1.98 ± 0.96	9.13 ± 0.38	0.22
2018-04-29	58237.108	APOGEE-S	1502	102	-1.45 ± 0.94	9.19 ± 0.37	0.22
2019-01-21	58504.318	APOGEE-S	2503	166	-1.71 ± 0.87	10.92 ± 0.37	0.37
2019-01-22	58505.332	APOGEE-S	3003	200	-1.78 ± 0.84	10.86 ± 0.36	0.37
2019-01-23	58506.369	APOGEE-S	2002	141	-1.66 ± 0.88	10.96 ± 0.37	0.37
2019-01-25	58508.291	APOGEE-S	2002	125	-1.95 ± 1.03	10.73 ± 0.42	0.37
2019-01-26	58509.297	APOGEE-S	2503	137	-1.67 ± 0.89	10.80 ± 0.38	0.38
2019-03-21	58563.120	APOGEE-S	1502	132	-2.00 ± 0.84	11.32 ± 0.37	0.41
2019-03-22	58564.127	APOGEE-S	2002	160	-1.71 ± 0.86	11.56 ± 0.37	0.41
2023-04-27	60061.112	APOGEE-S	447	58	-1.86 ± 1.42	10.04 ± 0.55	0.26
2019-04-04	58577.137	UVES	1200	72	-1.56 ± 0.10	11.53 ± 0.20	0.41
2019-04-25	58598.051	UVES	1200	59	-1.77 ± 0.11	11.68 ± 0.22	0.43
2019-05-20	58623.018	UVES	1200	106	-1.22 ± 0.09	11.63 ± 0.18	0.44
2019-07-14	58678.053	UVES	1200	124	-1.36 ± 0.08	11.67 ± 0.16	0.47
2021-08-07	59433.991	UVES	1400	89	-1.53 ± 0.09	8.19 ± 0.18	0.90
2022-07-12	59772.006	UVES	1680	63	-1.46 ± 0.10	8.17 ± 0.20	0.09
2022-07-13	59773.994	UVES	1680	72	-2.08 ± 0.10	8.20 ± 0.20	0.09
2022-08-03	59794.010	UVES	1680	92	-1.61 ± 0.10	8.22 ± 0.20	0.10

$\Delta\lambda$ are the separations of the Zeeman components from the line center, k is a constant equal to $4.671 \times 10^{-13} \text{ \AA}^{-1} \text{ G}^{-1}$, and g_{eff} is the effective Landé factor. This method is an approximation for all but the simplest cases, but it nonetheless provides $\langle B \rangle$ estimates that are roughly consistent for a variety of Zeeman patterns.

The analysis focused on just one line in the H -band – Ce III 16133.17 Å. In addition to being one of the strongest, most isolated, and most clearly split lines covered, the Ce III strength is relatively constant from epoch to epoch unlike some other ions. Several other lines meet the same criteria, but unfortunately their carrier ion(s) is unidentified, with no likely counterparts in the available atomic data.

Fe II 6149.246 Å is widely regarded as the ground truth for $\langle B \rangle$ measurement (Mathys 2017), and indeed is the most likely RMSL to be present in Ap/Bp spectra due to having $J = 0.5$ for both levels of the transition, $g_{\text{lo}} = 0$, and $g_{\text{hi}} = 2.7$. This combination of J and g results in a simple Zeeman doublet pattern that is highly sensitive to field strength due to g_{hi} taking the place of g_{eff} in the aforementioned equation. Unfortunately, the line is problematic in this case. First of all, the blending is quite severe, with possible contributions from an Sm II line at 6149.060 Å and with definite contributions from an unidentified line at 6148.85 Å. Although satisfactory fits to the Fe II+Sm II+unknown blend can often be achieved for stars with weaker magnetic fields by treating the unknown line as a single wide Gaussian (e.g. Giarrusso et al. 2022), that approximation is in this case complicated by the strong and variable surface magnetic

field strength, the unknown Zeeman pattern of the 6148.85 Å line, the variable line strengths of most ions, and the fact that some ions exhibit significant phase lags in the variability with respect to others.

Instead, $\langle B \rangle$ was estimated from the UVES spectra using ten isolated REE lines that were present during all epochs and widely split into quasi-triplet features. This included four Pr III lines (6429, 6500, 7113, 8854 Å), five Dy II lines (8417, 8473, 8549, 8656, 8716 Å), and one Dy III line (6118.4 Å). Figure 1 shows examples of line profile fitting in the two APOGEE spectra and two UVES spectra that represent the observed $\langle B \rangle$ extremes from each data set.

3.2 Rotation Period

The $\langle B \rangle$ measurements from the APOGEE spectra show that the field strength of CPD-62° 2717 increased steadily from around ~8.7 kG in February of 2018 up to ~11.5 kG in late March of 2019. This trend continued in the UVES spectra from April, May, and July of 2019, with $\langle B \rangle$ hovering around 11.6 kG. More than two years passed before the next UVES observation in August of 2021, and by then $\langle B \rangle$ reached a new low of 8.2 kG. The three spectra from July–August of 2022 were all but identical to the 2021 spectrum, with $\langle B \rangle$ still hovering around the observed minimum of 8.2 kG. The most recent APOGEE observation from late April of 2023 indicated that $\langle B \rangle$ had climbed back up to ~10.0 kG once again.

All of the above indicates an exceedingly long rotation period for

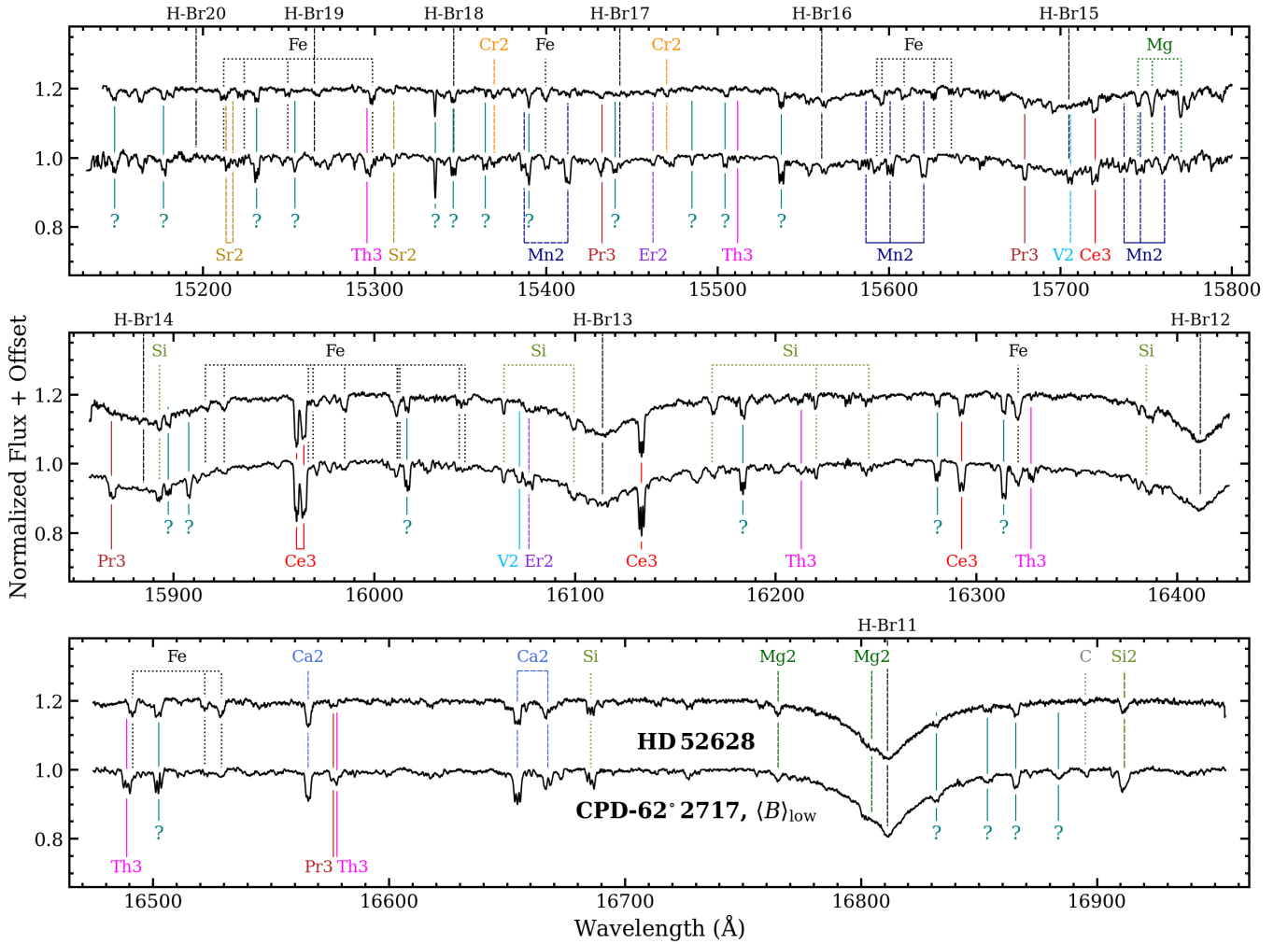


Figure 3. The mean APOGEE $\langle B \rangle_{\text{low}}$ spectrum of CPD-62° 2717 compared to the mean APOGEE spectrum of HD 52628. Most of the strong absorption lines are labeled, with “H-Br11–20” indicating the hydrogen Brackett series lines and with question marks indicating lines that lack likely counterparts in the existing atomic data. For conciseness, ionization stages are omitted from neutral elements labels and given as integers for ionized elements.

CPD-62° 2717, and this is demonstrated in Figure 2. The upper panel shows the $\langle B \rangle$ measurements as a function of time, with dotted line boxes enclosing epoch groupings in which the combined spectra will be used for the remainder of this paper. The 2023 April APOGEE spectrum is not included in these groupings since it has considerably lower S/N than the other APOGEE spectra and since the associated intermediate $\langle B \rangle$ it does not fit coherently with either the $\langle B \rangle_{\text{low}}$ nor $\langle B \rangle_{\text{hi}}$ epoch groupings.

The best-fitting sine curve to the $\langle B \rangle$ measurements is shown in the lower panel of Figure 2, and it is admittedly tentative due to the sparseness of the observations and the large gaps in phase coverage. Nonetheless, the available data indicate $P_{\text{rot}} \approx 1760$ days (4.82 years), which places CPD-62° 2717 firmly into the class of super-slow-rotating Ap stars (ssrAp; Ap stars with $P_{\text{rot}} > 50$ days) that was recently defined by Mathys (2020). Considering that we found $P_{\text{rot}} \approx 1765$ days prior to the APOGEE spectrum from 2023 April, addition of that data point merely validated rather than changed the results.

3.3 Radial Velocities

As for the radial velocities, we found an average from the APOGEE spectra of $v_r = -1.91 \pm 0.99 \text{ km s}^{-1}$ (after applying heliocentric corrections) and a far more precise average of $v_r = -1.57 \pm 0.10 \text{ km s}^{-1}$ from the UVES spectra, for an overall average of $v_r = -1.83 \pm 0.83 \text{ km s}^{-1}$. The individual epoch measurements range from -2.53 to -1.22 km s^{-1} , but they all agree to within the error bars such that we have no reason to suspect CPD-62° 2717 having a binary companion. If it does, either the mass ratio must be very low or the orbital period very long.

Table 1 provides a summary of the observations of CPD-62° 2717, including observation dates, Modified Julian Dates (MJD) at mid-exposure, instruments used, exposure times, signal-to-noise ratios (S/N; as reported by the APOGEE and UVES pipelines), heliocentric radial velocities (v_r ; in km s^{-1}), $\langle B \rangle$ estimates, and approximate rotation phases (ϕ_{rot}).

3.4 TESS Lightcurve

Considering the remarkably high fraction of roAp stars found among the ssrAp stars (22%, versus 3% for non-ssrAp stars) by Mathys et al. (2020), it is natural to wonder if CPD-62° 2717 might also be a short-period pulsator and whether this could be discovered from Transiting Exoplanet Survey Satellite (TESS; Ricker et al. 2015) data. To date, CPD-62° 2717 has been observed in three TESS sectors (1800 s cadence in sector 11 in 2019 and 600 s cadence in sectors 37 and 38 in 2021).

Despite the cadences not being well-suited for detecting very short period variability, we used the LIGHTKURVE (Lightkurve Collaboration et al. 2018) package to download the associated lightcurves, all of which show perfectly repeating variability with an amplitude of a few percent and with a period of 0.5772 days as determined using the time series analysis code PERIOD04 (Lenz & Breger 2005). This period is several dozen times longer than the longest known roAp pulsation period and can likely be attributed a nearby neighbor (22'' separation; similar to the size of a TESS pixel) of comparable brightness (SIMBAD quotes $V = 10.02$ for TYC 8979-1364-1 and $V = 10.42$ for CPD-62° 2717) that is almost certainly an RR Lyrae variable. Given the lack of short-cadence observations and contamination of the existing observations by the neighbor star, it is therefore difficult/impossible to determine whether or not CPD-62° 2717 is a roAp star based on the existing TESS data.

4 H-BAND SPECTRA

In the opinion of the first author of this paper, who has spent a great deal of time visually inspecting spectra of peculiar stars observed by the APOGEE instruments, CPD-62° 2717 is not particularly remarkable at first glance. Admittedly, the absorption lines are all magnetically split, thus placing CPD-62° 2717 in the select group of just a few hundred stars known to exhibit RMSL. However, the APOGEE Ap/Bp star sample contains a few dozen stars with $\langle B \rangle > 8$ kG and up to 24 kG. Further, whereas many of the strongest observed lines in the CPD-62° 2717 spectra have no counterparts in the atomic data and instead remain unidentified, the same is true for several hundred other Ap/Bp stars in the APOGEE sample.

These sentiments are demonstrated in Figure 3, which displays the mean $\langle B \rangle_{\text{low}}$ APOGEE spectrum of CPD-62° 2717 along with the mean APOGEE spectrum of HD 52628, which is the closest thing to a spectroscopic twin of CPD-62° 2717 that we could find. The similarity is striking in terms of both line content and line strengths, and the magnetic field strengths are also in the same ballpark ($\langle B \rangle \sim 7$ kG for HD 52628). As is typical in the H -band spectra of Ap stars, the three strongest metal lines for both stars are Ce III 15961, 15965, and 16133 Å. For CPD-62° 2717 and HD 52628, the next strongest lines are Ca II 16566 and 16654 Å, which are followed by numerous unidentified lines that we strongly suspect the majority of can be attributed to a single ion, most likely an REE3. Despite being unidentified, the unknown line at 15335 Å is particularly useful given that it clearly has an extremely low effective Landé factor. The line thus appears as a narrow spike in the case of slow rotation, and in addition to setting an upper limit on $v \sin i$, the line can be used to confirm magnetic splitting in other lines, all of which have considerably higher effective Landé factors.

Some of the weaker lines that can actually be identified and that are in common between CPD-62° 2717 and HD 52628 include a C I line, a few dozen Si I and Fe I lines, an Si II line, a few Mg II lines, several Pr III lines, and a few weak Er II lines. It was not until preparing this

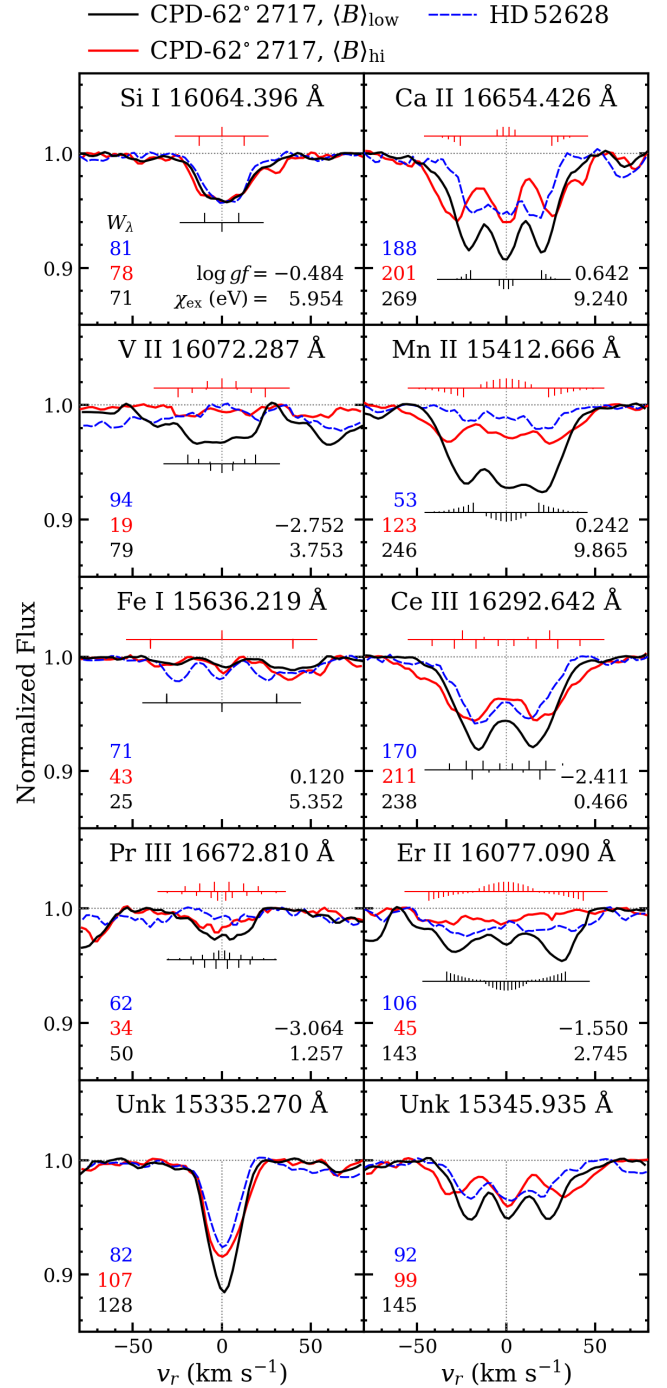


Figure 4. Comparison of line profiles from the mean APOGEE $\langle B \rangle_{\text{low}}$ and $\langle B \rangle_{\text{hi}}$ spectra of CPD-62° 2717 and the mean APOGEE spectrum of HD 52628. In cases where the lines could be identified, the individual π and σ_{\pm} components are shown above and below the line profiles, with the upper Zeeman pattern scaled horizontally to the $\langle B \rangle \sim 11.0$ kG of CPD-62° 2717 in $\langle B \rangle_{\text{hi}}$ mode, and with the lower, reflected Zeeman pattern scaled to the $\langle B \rangle \sim 8.8$ kG of CPD-62° 2717 in $\langle B \rangle_{\text{low}}$ mode. Direct summation equivalent widths (W_{λ} , in mÅ) are given below and left of each line profile, and oscillator strengths ($\log gf$) and excitation energies (χ_{ex} , in eV) are given below and right of the line profiles.

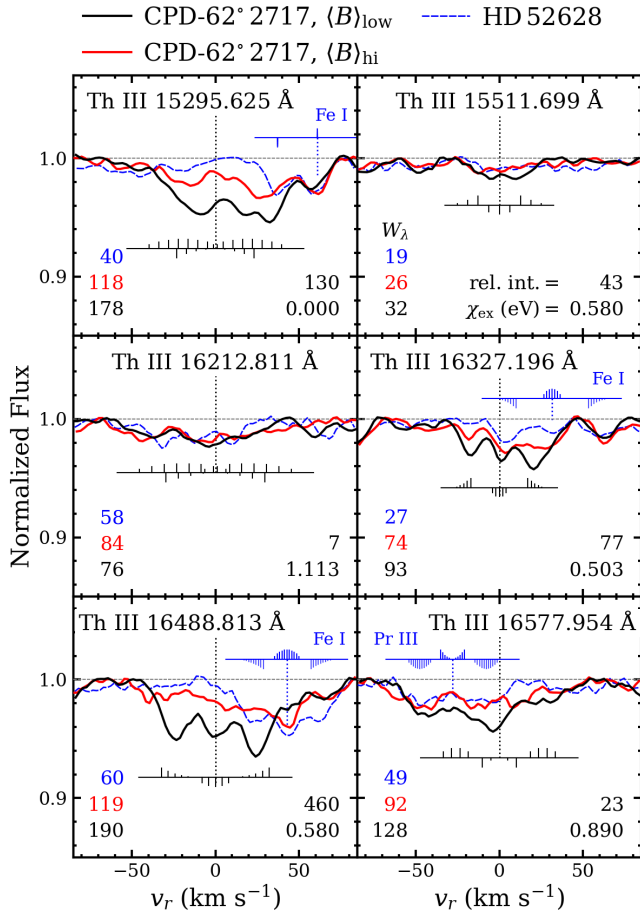


Figure 5. The H -band Th III lines of CPD-62° 2717. Meanings are mostly the same as in Figure 4 except for a few details. Relative intensities from Redman et al. (2014) are given rather than $\log g f$, and to demonstrate that the Th III lines are not actually present in the HD 52628 spectrum, the Zeeman patterns of nearby Fe I and Pr III lines are shown above the line profiles (scaled horizontally for the 7.0 kG of HD 52628).

paper that we recognized the presence of the latter, and if not for the subject matter at hand, the Er II lines at 15462 Å and 16077 Å would represent the heaviest metal ever detected in stellar H -band spectra (regardless of spectral type).

Despite the apparent similarity of CPD-62° 2717 and HD 52628 when the spectra are viewed widely as in Figure 3, it is the subtle differences that set CPD-62° 2717 apart from any other APOGEE-observed stars that we are aware of.

Figure 4 provides a detailed view of individual lines in the spectra displayed in Figure 3 as well as in the $\langle B \rangle_{hi}$ spectrum of CPD-62° 2717. Si I 16064 Å is one of the few low- g_{eff} lines present in the CPD-62° 2717 spectra (along with the unknown 15335 Å line) for which magnetic splitting is not resolved at this combination of resolving power and magnetic field strength. Si I is also one of the few ions whose line strengths are relatively stable across the $\langle B \rangle_{low}$ and $\langle B \rangle_{hi}$ phases of CPD-62° 2717.

Beginning with Ca II, the large degree of variability as a function of rotation phase of some of the other ions becomes apparent. The behavior of V II and Mn II is particularly noteworthy in this context due to the dramatic variability. The line strengths of both ions change by a factor of two or more between $\langle B \rangle_{low}$ and $\langle B \rangle_{hi}$ phases, and the V II lines are essentially absent altogether from the $\langle B \rangle_{hi}$ spectrum.

As for Fe I, the lines are quite weak in the CPD-62° 2717 spectra, but a hint can be seen for of variability that is anti-phased with respect to V II and Mn II. This is possibly true for Si I as well.

The variability of the known and suspected REE is also a mixed bag, differing from ion to ion. Whereas Pr III, Ce III, and the unknown lines are relatively stable, Er II follows the trend established by V II and Mn II in terms of the lines all but disappearing during $\langle B \rangle_{hi}$ phases.

5 H -BAND TH III DETECTION

As remarkable as CPD-62° 2717 is without even mentioning thorium, Figure 5 demonstrates why the star is particularly special. Six of the seven Th III lines from Redman et al. (2014) that are covered by APOGEE spectra are shown. The Th III line that is not shown and that can be considered a non-detection falls at a vacuum rest wavelength of 16064.373 Å. In addition to Redman et al. (2014) having quoted a relative intensity of just 7 (a very low number in this context) for this line, it would be fully blended with Si I 16064.396 Å even if it was stronger. Redman et al. (2014) also quoted a relative intensity of 7 for the Th III line at 16212.811 Å, and we consider it a tentative detection at best.

As for the five Th III lines with relative intensities > 7 , they all appear to be present despite some level of blending in most cases. The Redman et al. (2014) linelist suggests the 15511.699 Å and 16577.954 Å lines should be quite weak, and indeed they are. Likewise, the 15295.625 Å, 16327.196 Å, 16488.813 Å lines should be the strongest H -band Th III features, and indeed they are blatantly present albeit with the red wing of the 15295.625 Å line being blended with one of the strongest Fe I lines covered by the APOGEE spectra. For the 16327.196 Å and 16488.813 Å lines in particular, the agreement between the expected and observed central positions, relative strengths, and Zeeman patterns during the $\langle B \rangle_{low}$ phases of CPD-62° 2717 leaves little doubt as to the Th III identification.

Similar to V II, Mn II, and Er II, the contributions from Th III are sufficiently weak in the $\langle B \rangle_{hi}$ spectra of CPD-62° 2717 that they likely would not have been acknowledged were it not for the $\langle B \rangle_{low}$ APOGEE observations. It could therefore be argued that CPD-62° 2717 is perhaps not as unique as this paper implies, and that the observation timing has simply been unfortunate for the other hundreds of highly peculiar Ap stars that APOGEE has observed. As it stands for now however, CPD-62° 2717 can just as easily be considered a needle in a haystack due to an obviously severe Th III over-abundance patch on its surface along with a magnetic field strength suitable for confirmation via Zeeman pattern matches.

6 OPTICAL TH III DETECTION

Whereas the H -band spectra of CPD-62° 2717 merely provided hints about the degree of peculiarity at hand, the optical spectra make it clear that ‘extreme’ is a proper qualifier. All of the trends hinted at by the H -band are confirmed, and we begin our discussion of the optical spectra by getting right to the point. Th III lines are not only present in the UVES spectra of CPD-62° 2717, they are numerous.

The optical Th III linelist provides atomic data for a total of 82 lines between 5700–9100 Å. Of these 82 lines, we see no evidence in the CPD-62° 2717 spectra of the 38 with excitation energies higher than 2 eV and/or with oscillator strengths less than -3.05 . Another 14 lines are either contaminated by telluric absorption during all observed epochs or else fall at roughly the same wavelengths of

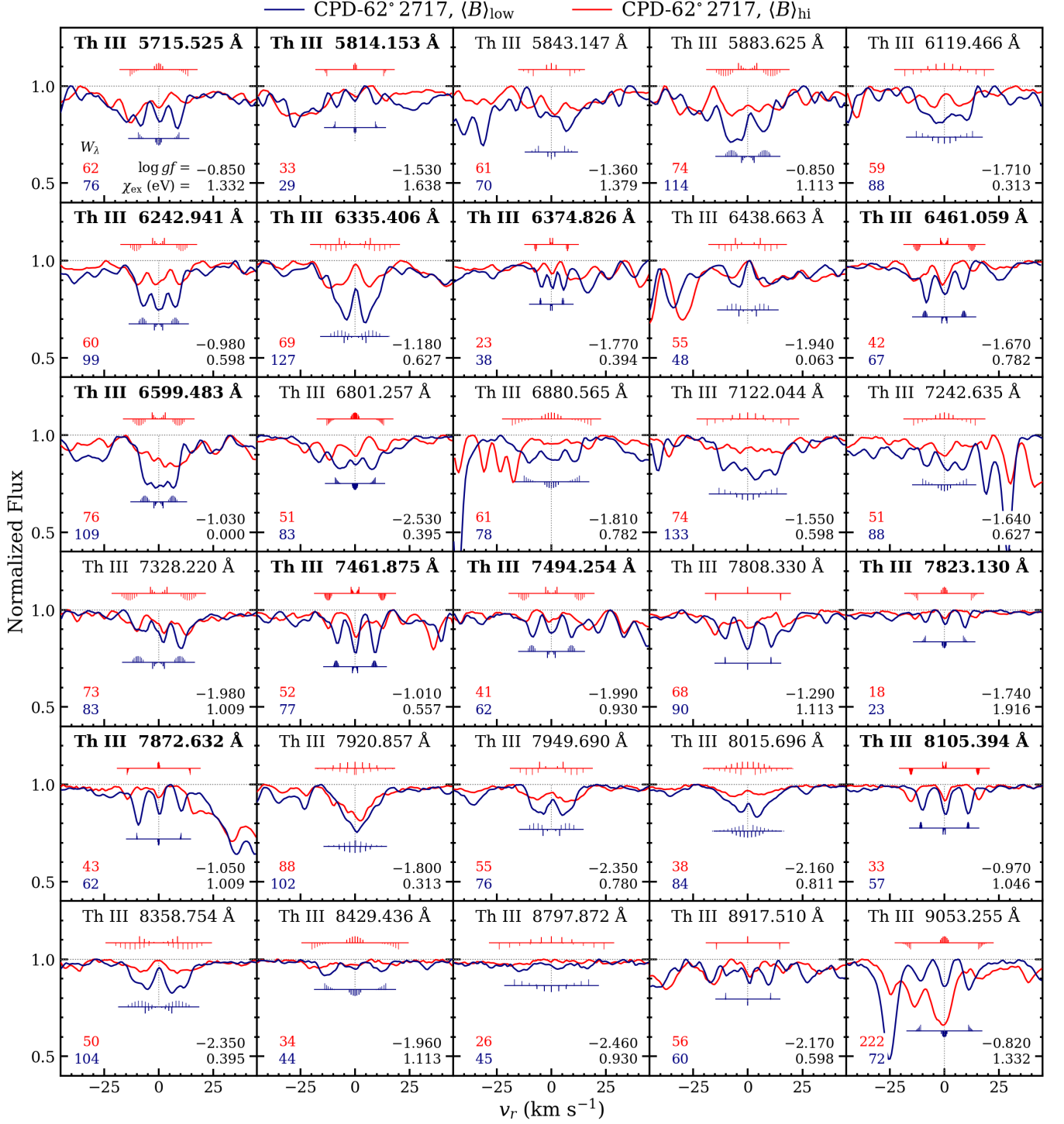


Figure 6. The best evidence to date of thorium in the atmosphere of an Ap star. Each panel shows Th III line profiles from the mean UVES $\langle B \rangle_{\text{low}}$ (navy) and $\langle B \rangle_{\text{hi}}$ (red) spectra of CPD-62° 2717. The associated Zeeman patterns are shown above and below each line profile pair and scaled to $\langle B \rangle = 11.6$ kG (upper Zeeman pattern) and $\langle B \rangle = 8.2$ kG (reflected lower Zeeman pattern). Bold font of the labels above the line profiles indicates cases of minimally blended lines with relatively high $\log gf$ and for which the observed Zeeman patterns match those expected from the atomic data. As in Figure 4, direct summation equivalent widths, oscillator strengths, and excitation energies are given below the line profiles.

stronger lines from other ions. In Figure 6, the line profiles of the remaining 30 Th III lines are displayed as they appear in the UVES $\langle B \rangle_{\text{low}}$ and $\langle B \rangle_{\text{hi}}$ spectra of CPD-62° 2717. Some evidence can be seen for the presence of all of them, despite most being blended to some extent.

Among the detected Th III lines are a resonance line at 6599.483 Å (see Fig. 6) that has an oscillator strength of $\log gf = -1.030$ and that should be among the strongest Th III lines between 5700–9100 Å. Indeed it is one of them. The equivalent width of the 6599 Å line in the $\langle B \rangle_{\text{low}}$ is topped only by that of the Th III lines at 6335 Å and 7122.044 Å, and the latter is almost certainly blended with an unknown line. The most likely contaminants of the 6599 Å line are the Fe II lines at 6599.804 Å ($\log gf = -2.883$, $\chi_{\text{ex}} = 7.6973$ eV) and 6600.025 Å ($\log gf = +0.295$, $\chi_{\text{ex}} = 11.0164$ eV), each of which could overlap the Th III line sufficiently fast stellar rotation or sufficient magnetic splitting. In the case of CPD-62° 2717 however, the contributions to Th III 6599 Å from Fe II can be deduced to be minimal. Other Fe II lines with longer wavelengths (and hence less chances of blending with REE lines), similar energy levels, and even higher $\log gf$ are either absent from the spectra or exceedingly weak.

As noted above, the 6335.406 Å line (see Fig. 6) is also among the strongest Th III features in the CPD-62° 2717 spectra. For other Ap stars, its presence can easily be mistaken for Fe I 6335.330 Å ($\log gf = -2.177$, $\chi_{\text{ex}} = 2.1979$ eV), but for CPD-62° 2717, the observed central wavelength, Zeeman pattern, and symmetry of the feature all indicate that the contribution from Fe I is negligible. Similar to the case of Th III 6599 Å, this can also be confirmed through inspection of Fe I lines that should be even stronger than the 6335.330 Å line.

The 6243 Å line (see Fig. 6) is another of the most obvious Th III features, and for CPD-62° 2717, it appears to be a rare example (regardless of ion) of a mostly blend-free line during both the $\langle B \rangle_{\text{low}}$ and $\langle B \rangle_{\text{hi}}$ phases. Another that fits in the same category and that was also exquisitely split during all of the UVES observations is Th III 8105.394 Å line. The region around this line can be mildly contaminated by telluric absorption under poor observations conditions, but our linelist includes no likely stellar absorption contaminants in the vicinity. The results displayed in Figure 2 can in fact be closely duplicated by applying the same analysis described in Section 3 to Th III 8105 Å. This is also true for Th III 6243, 7461, and 7823 Å. Most of the other Th III lines become blended with neighboring during $\langle B \rangle_{\text{hi}}$ phases due to increased widths of the RMSL.

There are a few more details worth mentioning before moving on. The Th III lines at 6881, 7243, 7921, and 9053 Å (see Fig. 6) all fall in regions of likely telluric contamination. The 7921 Å line is the most magnetically insensitive of the displayed Th III lines, and although a weak telluric feature is almost certainly blended with the observed feature, the lack of RMSL nonetheless supports the identification of the line as Th III.

7 OTHER ELEMENTS IN THE OPTICAL

7.1 Light Elements

Figure 7 shows profiles of lines from 35 ions that are likely or definitely present in the 5700–9000 Å range in the UVES spectra of CPD-62° 2717. The identifications are based on reasonable matches between the observed and expected central positions, relative intensities, and Zeeman patterns of numerous lines in most cases.

The lightest metal lines whose presence can be confirmed are the O I 7772, 7774, and 7775 Å triplet, and although quite weak

and blended in the case of O I 7775 Å, the identifications can be confirmed by the widely split 7772 Å and 7774 Å lines. Mg, Si, Ca, Sc, and Ti are the next lightest elements present, albeit represented by just a few lines each. With the exceptions of Sc and Ti, for which lines from the neutral variety are not detected, the singly-ionized variety is far stronger than the neutral. Si II and Ca II in particular are likely to be overabundant on the surface of CPD-62° 2717 based on comparison to archival UVES spectra of cool Ap stars. By that same argument, Ti II may be close to solar if not slightly below.

As for the iron peak elements, the trends established in the H -band spectra of CPD-62° 2717 are repeated in the optical. Namely, lines from V II and Mn II are abnormally strong during the $\langle B \rangle_{\text{low}}$ phases. This seems to be a quite rare abundance anomaly. We’ve been unable to identify any other Ap star whose archival UVES spectra shows stronger V II lines than those of CPD-62° 2717. The lines are simply not present in the spectra of most Ap stars. Mn II lines on the other hand are often present, just not at the strengths observed in the $\langle B \rangle_{\text{low}}$ phase of CPD-62° 2717.

Note that the identification of the RMSL around 6016.7 Å as Mn I is tentative. In addition to the positions of the magnetically split components being slightly offset from expectations (possibly due to blending), a few other Mn I lines (6013.510 Å and 6021.820 Å) that should be of comparable strength do not seem to be present. Further, whereas the variability trend of the possible Mn I 6016.670 Å line follows that of the Mn II lines, that does not necessarily confirm the identification. We can only identify just over half of the lines in a given wavelength range, meaning that at least one (more likely several) important ion is missing from our linelist.

Similar to PS, unblended Fe lines are not easy to find in the spectra of CPD-62° 2717. Considering the long-running debate over whether Fe was missing from the atmosphere of PS (Przybylski 1977), we suspect that Przybylski would be amused to see another example of this, though with a far stronger magnetic field in this case. Fe is certainly present of course, and based again on comparison to archival UVES spectra of other Ap stars for which abundances have been estimated, Fe I may be slightly underabundant with respect to Solar, while Fe II may be slightly overabundant. Whatever the case, one thing is certain: RMSL from heavier elements are far more obvious in the 5700–9000 Å region.

Sr II is the only ion between the iron peak and the REE that we’ve been able to confirm the presence of in the CPD-62° 2717 spectra, and it appears to be severely enhanced as is empirically expected for Ap stars in this temperature regime. The Sr II resonance lines at 4077.709 Å and 4215.519 Å are among the strongest metal features in the blue UVES spectra, and another Sr II line at 4305.443 Å is also present and quite strong. As for the 5700–9000 Å region, the Sr II lines at 8506.006 Å ($\chi_{\text{ex}} = 6.915$ eV, $\log gf = 0.270$, $g_{\text{eff}} = 0.83$) and 8689.298 Å ($\chi_{\text{ex}} = 6.950$ eV, $\log gf = 0.516$, $g_{\text{eff}} = 1.10$) are expected to be strongest and should be magnetically split in the case of CPD-62° 2717. Indeed, these lines appear to be present with the expected flux ratios (W_{λ} of Sr II 8689 Å is about twice that of Sr II 8506 Å) and also with the expected Zeeman patterns (quasi-triplets). However, unlike most of the other ions represented in Figure 7, we found that it was necessary to apply a 14.37 km s^{-1} velocity correction to the rest wavelengths quoted by VALD in order for the central components of the observed features to align with $v_r = 0$ (as in Figure 7 for Sr II 8689 Å). The cause of these wavelength discrepancies is unclear.

Although Y II and Ba II are often present in the spectra of cool Ap stars, with Ba II often accounting for several of the strongest metal lines in the optical, the spectra of CPD-62° 2717 show little to no evidence of these ions.

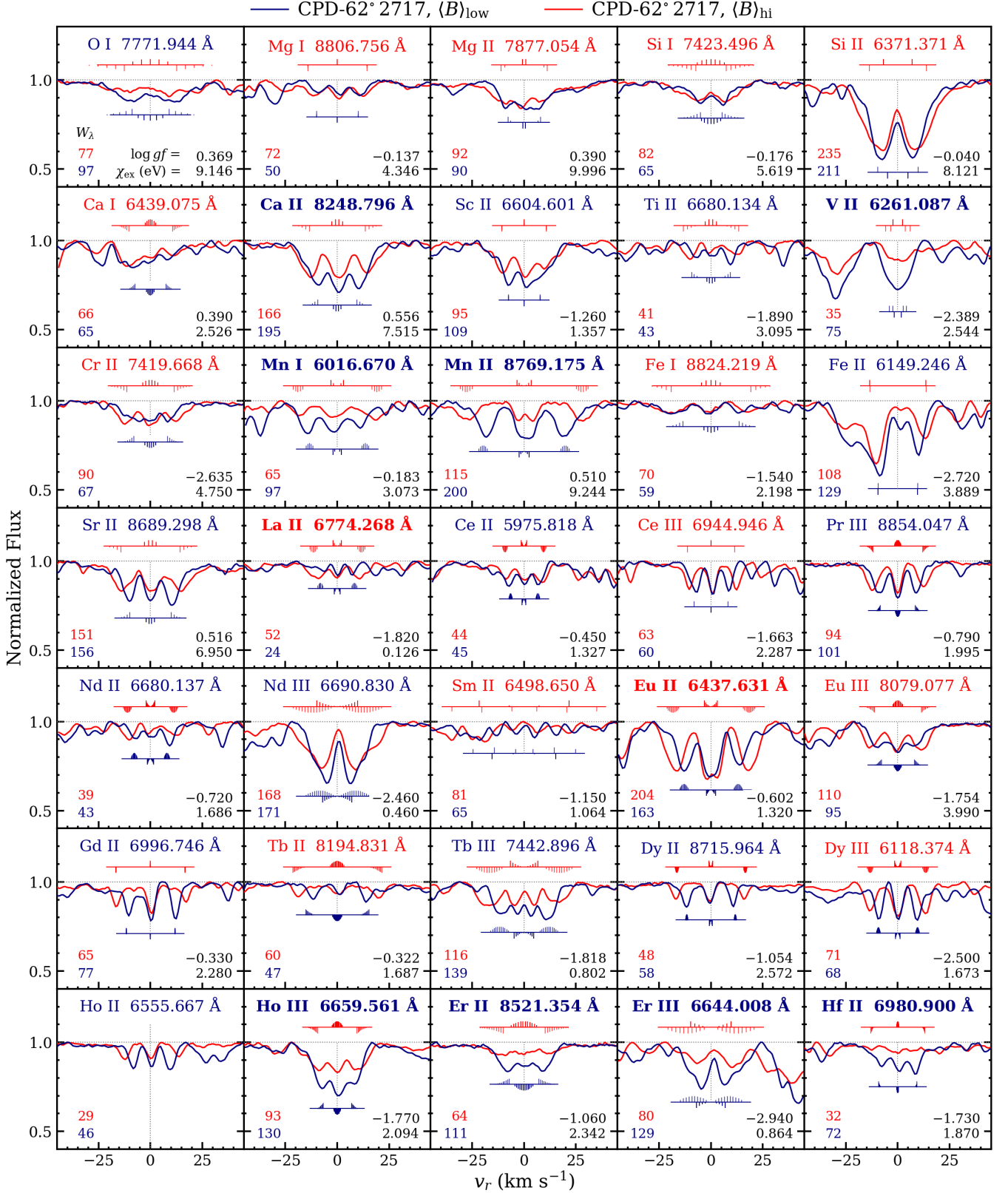


Figure 7. The periodic table of peculiar at $\lambda > 5700 \text{ \AA}$ in the UVES spectra of CPD-62° 2717. Meanings are mostly the same as in Figure 6. With the exception of Hf II, for which only one line seems to be present, each panel shows a representative line from an ion whose presence is supported by the central positions, relative intensities, and Zeeman patterns of > 1 and often numerous lines. The color coding of the ion & wavelength labels corresponds to the coloring of the spectra, such that for example if the line is strongest in the $\langle B \rangle_{\text{hi}}$ spectrum, the label is red. Bold font indicates cases of significant variability whereby the line strength changes by $> 25 \text{ m\AA}$ between the $\langle B \rangle_{\text{low}}$ and $\langle B \rangle_{\text{hi}}$ phases. Note that full atomic data is not available for the Ho II line (rest wavelength taken from Özdalgıç et al. 2019) and the quoted W_λ were measured manually.

7.2 Rare Earth Elements

Most of the REE are definitely present in the CPD-62° 2717 spectra, albeit with the light REE2 being quite weak. In particular, only a small handful of unblended RMSL from La II, Ce II, and Sm II can be found between 5700–9000 Å, while Pr II lines are exceedingly weak if not absent altogether. Nd II is far better represented and also more easily confirmed thanks to several relatively magnetically insensitive lines (e.g., Nd II 6580.930 Å, with $g_{\text{eff}} = 0.23$). Eu II is almost always strong in the spectra of cool Ap stars, and the situation is no different for CPD-62° 2717. However, the strengths of the Eu III lines (10 of which appear to be present) are particularly noteworthy since the same lines are absent from the spectra of PS and from most Ap stars in general.

It is worth noting that the observed positions of Sm II and Eu III lines in the CPD-62° 2717 spectra are systematically offset from the VALD wavelengths by about 3.5 km s^{-1} , and the velocities of the associated line in Figure 7 have been corrected by that value. Unlike the situation with Sr II (see Section 7.1), this may be due to Sm II and Eu III overabundance spots on the surface of CPD-62° 2717 whose locations strongly differ from those of the Pr and Dy lines used for radial velocity measurement.

Along with Th III, it is the contributions from heavy REE3 that set CPD-62° 2717 apart from other Ap stars. Lines from Dy II are numerous in the CPD-62° 2717, with at least 83 lines present and exquisitely split like the 8715.964 Å line shown in Figure 7. Of all the ions present, Dy II is actually the easiest to confirm, far easier than Fe for example. Other ions that fall into this category include Pr III (at least 43 RMSL), Gd II (at least 60 RMSL), and Tb III (at least 43 RMSL).

The Ho and Er lines of CPD-62° 2717 are also noteworthy considering that we are aware of no other Ap star for which they stronger. The only stars that we know of which even come close are the cool Ap stars HD 81588 and HD 143487 (which will be discussed in a subsequent section of this paper). Unfortunately, the Ho II, Ho III, and Er III linelists are quite limited, and some parts of the Er III linelist may in fact be erroneous given lines like the one at 5903.284 Å, for which the observed and expected splitting patterns and splitting widths are a severe mismatch.

Although VALD currently lacks atomic data for Ho II lines at wavelengths longer than 4212 Å, Özdalgıç et al. (2019) classified numerous lines up to 7000 Å as Ho II and Ho III. The most isolated and clearly split of the Ho II lines (6555.667 Å) from that work is shown in Figure 7. There are a few nearby lines that might show up in stellar spectra (Pr II 6555.609 Å, Ce I 6555.649 Å, and Mn II 6555.686 Å), but those lines are not expected to be present in the CPD-62° 2717 spectra given the weakness or non-detections of stronger lines of the associated ions. Further, the observed Zeeman pattern empirically indicates $g_{\text{eff}} \sim 1.2$, which is inconsistent with the other possible contaminants. Some of the other Ho II lines from Özdalgıç et al. (2019) that appear to be present in the > 5700 Å region of the CPD-62° 2717 spectra include 6985.076 Å (doublet pattern), 6976.756 Å (triplet), 6655.714 Å (triplet), 6208.607 Å (triplet), 6073.607 Å (triplet), 6060.207 Å (triplet), 6058.185 Å (triplet), 6022.252 Å (triplet), 6005.267 Å (doublet), 5993.057 Å (triplet), 5961.704 Å (triplet), 5961.195 Å (low- g_{eff} ?), 5904.277 Å (triplet), 5866.437 Å (triplet), and 5839.441 Å (triplet). Most of these lines are blended to some extent.

Surprisingly, we have found no evidence for lines from the heaviest REE – Tm, Yb, and Lu – in the CPD-62° 2717 spectra, or at least none that are not buried beneath a plethora of stronger lines.

7.3 Heavy Elements

The only element between the REE and thorium that seems to possibly be present is Hf II, which immediately follows the REE in the periodic table at $Z = 72$. There are depressions in the continuum at the positions of most of the Hf II lines with $\log gf > -2$ in the 5700–9000 Å region, but the nearly all of these suffer from blending. The Hf II 6980.900 Å line is the best example we could find and it too appears to be blended, with possible telluric contributions. However, our linelist includes no other likely candidates in the vicinity that would contribute to the observed feature. Furthermore, the variability of the possible Hf II line is quite similar to that of the heavy REE and Th III, such that Hf II may indeed be the primary contributor to the 6980.900 Å RMSL.

The weakness if not lack of Th II features in the CPD-62° 2717 spectra is somewhat surprising. Much like Hf II, there are depressions in the continuum at the positions of most of the Th II lines that are expected to be strongest, but only a few of them exhibit Zeeman patterns consistent with expectations. The essential non-detection of Th II does not necessarily hinder the Th III line identifications however. Praseodymium exhibits similar behavior, whereby lines from Pr II are weak/absent while lines from Pr III are among the strongest in the spectra.

This section would not be complete without mentioning uranium. Although it is expected to be present in stellar atmospheres and is likely to be enhanced in the atmosphere of CPD-62° 2717 given the thorium enhancement, we could find no solid evidence for U II lines in the spectra. The same argument from the last paragraph applies equally well here; if anything, we would expect to see lines of U III. It remains to be seen if some of the unknown lines in the optical spectra of CPD-62° 2717 can be attributed to U III, and although it is understandably a tall order, the need for a laboratory-determined U III linelist covering the entire optical wavelength regime has never been more urgent.

8 IS THE THORIUM PECULIARITY UNIQUE TO CPD-62° 2717?

Given the nature of the discovery at hand, the expectation that it is unlikely to be unique, and our failure to find further examples among the APOGEE Ap star sample, it was only prudent to search the ESO spectra archive for additional stars with Th III lines. In hopes of this search being aided by Zeeman coincidence statistics, we started by inspecting the UVES and/or HARPS spectra available for 57 of the 84 Ap/Bp stars known to exhibit the magnetically split components of the Fe II 6149 Å line (Bagnulo et al. 2003; Hubrig et al. 2005; Freyhammer et al. 2008; Elkin et al. 2010a, 2012; Mathys 2017). We also checked the archival spectra of numerous Ap/Bp stars that have been identified as particularly peculiar in the literature despite lack of RMSL. Considering the Gaia DR3 $T_{\text{eff}} < 6834$ K of CPD-62° 2717, we also included in our search the spectra of numerous stars for which $T_{\text{eff}} < 7500$ K has been estimated.

The quest for CPD-62° 2717 analogues was ultimately narrowed to just three stars – PS, HD 81588, and HD 143487. Archival UVES spectra of these stars are displayed in Figure 8 along with the mean $\langle B \rangle_{\text{low}}$ UVES spectrum of CPD-62° 2717 and a UVES spectrum of the relatively pedestrian roAp star HD 122970. The latter is included simply emphasize the extreme peculiarity of the others. but HD 122970 is also one of the few Ap stars for which a thorium abundance has been estimated; Ryabchikova et al. (2000) reported an upper limit on [Th/H] of +2.11 dex with respect to solar based on analysis of four Th II lines. We see no strong evidence for thorium lines in the spectra of this star.

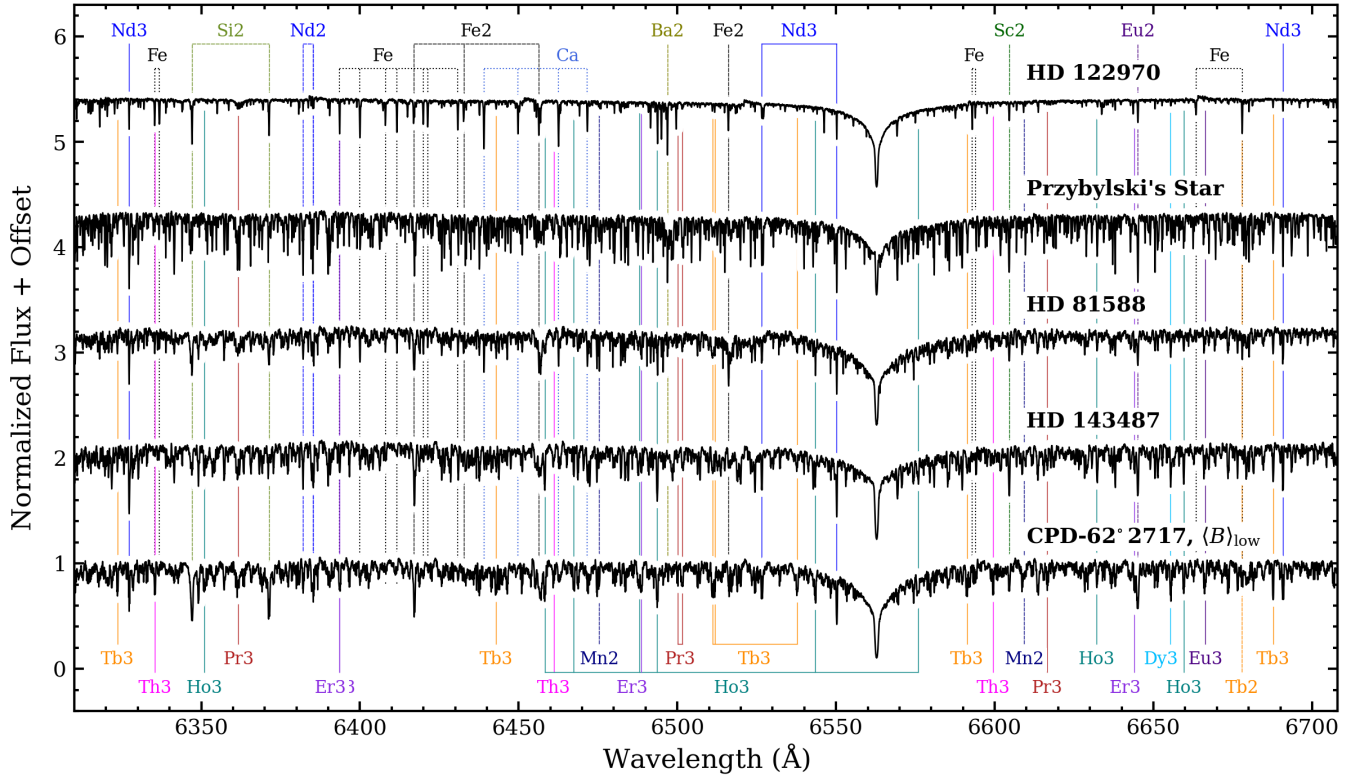


Figure 8. Comparison of the mean UVES $\langle B \rangle_{\text{low}}$ spectrum of CPD-62° 2717 to archival UVES spectra of other Ap stars that we identified as possibly exhibiting the Th III lines.

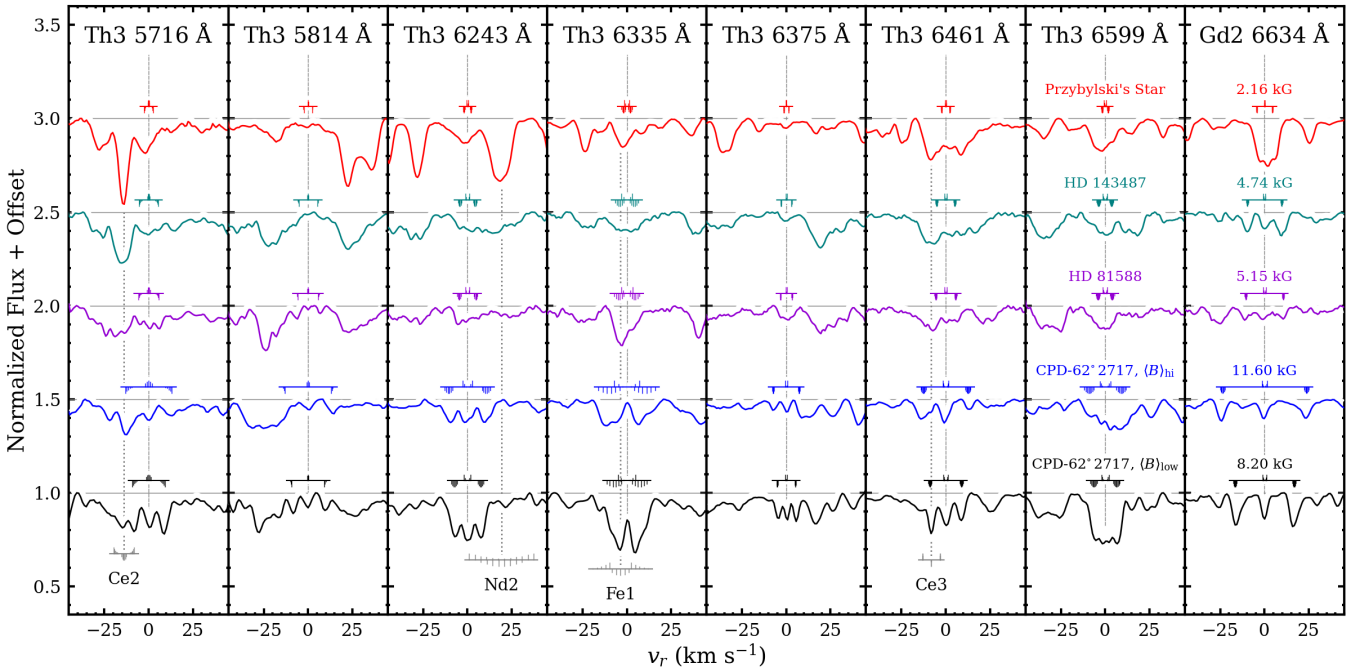


Figure 9. Comparison of Th III line profiles of CPD-62° 2717, HD 81588, HD 143487, and Przybylski's Star. The magnetically sensitive ($g_{\text{eff}} = 2.2$) Gd II 6634 Å line is also shown for context, since its magnetically split components are resolved in the spectra of all four stars.

All of the spectra displayed in Figure 8 have the same $R = 107\,000$ as those of CPD-62° 2717, and the spectra of HD 122970 and PS also cover the same wavelength range (5655–9464 Å) as those of CPD-62° 2717. The wavelength coverage (4959–7071 Å) of the HD 81588 and HD 143487 spectra unfortunately does not extend as far to the red and thus does not cover isolated Th III features such as the 8105 Å line. The observation of HD 122970 took place on 2008 August 3 and achieved S/N= 168 in a 500 s exposure. Numerous ESO archive spectra are available for PS, but since we didn’t see much evidence of temporal variability, we simply make use of the UVES observation from 2006 January 14, which achieved S/N= 267 in a 680 s exposure. The only UVES observation of HD 81588 took place on 2008 February 19 and achieved S/N= 330 in a 2200 s exposure. Four UVES spectra from 2007–2010 are available for HD 143487, and due to the associated lack of significant spectroscopic variability, we simply make use of the highest-S/N spectrum that was obtained on 2010 June 27 and that achieved S/N= 325 in a 3720 s exposure.

We could not help but notice that the four archival UVES spectra of HD 143487 show $> 10 \text{ km s}^{-1}$ radial velocity variations, with the 2007 and 2010 observations having $v_r \sim -25 \text{ km s}^{-1}$ and with the two 2008 observations having $v_r \sim -16 \text{ km s}^{-1}$, thus implying that it is a member of a binary system. This was also noticed by the Gaia collaboration¹, who found it to be single-lined spectroscopic binary (SB1) with a long 1354 day orbital period. Likewise, the UVES spectra show no evidence of a second set of lines.

In Figure 8, lines that are strong for typical cool Ap stars like HD 122970 are labeled along the top. With just a few exceptions, those same features are either absent, weak, or unrecognizable due to blending for the other stars. PS is well known as the most peculiar Ap star, and one does not need to be an expert in this genre to recognize why from a glance at Figure 8. Only a few of the strong lines of PS are labeled, but the majority of the unlabeled ones can be attributed to light REE2 (with particularly numerous contributions from Ce II, Nd II, and Sm II), light REE3, or to ions that are missing from existing linelists. Given that blank continuum regions in optical spectra of PS are rare (if not non-existent), it was inevitable that PS would be included in this discussion. There are simply local minima everywhere, and the presence of Th III (and just about any ion for that matter) cannot be ruled out.

Given the sparse literature mentions of HD 81588 and HD 143487, the degree of peculiarity of these stars came as somewhat of a surprise. Both stars are close spectroscopic analogues of CPD-62° 2717, and they are in fact the only examples we could find of Ho III and Er III line strengths even remotely close to those of CPD-62° 2717. All three stars are more extreme than PS in that respect.

The only study we are aware of that specifically discussed HD 81588 was Elkin et al. (2012), and these authors noted that the star “showed a highly peculiar spectrum with strong rare earth element lines of Nd III and Pr III.”. They also estimated $T_{\text{eff}} = 7400 \text{ K}$, thus putting HD 81588 near the extreme cool end of the Ap star temperature distribution. The Fe II 6149 Å line was found to be magnetically split with an implied $\langle B \rangle = 2.4 \pm 0.2 \text{ kG}$. We confirmed this to be the case in the UVES spectrum as well, but we also found that the $\langle B \rangle$ implied by virtually all of the other RMSL (most of which are REE lines) was more than double that of Fe II at $\sim 5.2 \text{ kG}$. This very large discrepancy is likely caused by significantly highly inhomogeneous distributions of Fe and REE on the surface of HD 81588, which results in a different weighting of the local field intensities in the averaging over the visible stellar disk.

HD 143487 was first specifically mentioned in the literature by Freyhammer et al. (2008), and in this case, splitting of the Fe II 6149 Å line indicated $\langle B \rangle = 4.23 \pm 0.07 \text{ kG}$. These authors also reported $T_{\text{eff}} = 6930 \text{ K}$ for HD 143487, thus also placing it toward the lower limit of T_{eff} for Ap stars and making it comparable to CPD-62° 2717, PS, and HD 81588. Similar to the case of HD 81588, Freyhammer et al. (2008) also pointed out that the “spectrum of HD 143487 is highly peculiar and, e.g. Pr, Nd are among the strongest of this study.” Elkin et al. (2010b) subsequently discovered that HD 143487 is a roAp star with an 8.8 minute pulsation period, and this period was then refined to 9.63 minutes by Kochukhov et al. (2013).

The two strong Th III lines at 6335 Å and 6599 Å are labeled along the bottom of Figure 8, and only for CPD-62° 2717 are they obvious. In order to check for their presence in the other stars, it is necessary to view the line profiles in detail. Figure 9 does just that, showing six of the Th III lines that are covered by the spectra of all four stars and that are clearly split in the CPD-62° 2717 spectra. The Gd II 6634 Å line is also included for context, since its magnetically split components are resolved at $R = 107\,000$ for all four stars. In the large upper panels, the Zeeman patterns above each line profile have been scaled horizontally according to the $\langle B \rangle$ values given in the Gd II panel at far right. For HD 81588, the $\langle B \rangle$ implied by REE lines has been adopted. When it was possible to identify blended features (usually it was not possible; e.g., the features right of Th III 6375 Å and left of Th III 6599 Å), the associated Zeeman patterns are shown along the bottom of the larger panels of Figure 9, scaled for $\langle B \rangle = 8.2 \text{ kG}$.

For PS, the Th III lines all appear to be partial blends; only for the two weakest lines (5814 Å and 6375 Å) do local minima coincide closely with the Th III wavelengths. The evidence for Th III is slightly better for HD 143487 considering that a local minimum coincides with Th III 6599 Å and also that the blue triplet component of Th III 6243 Å appears possibly to be resolved.

HD 81588 on the other hand shows quite convincing evidence of Th III. The magnetic splitting of the 5716 Å and 5814 Å lines appears to be resolved, and we are unaware of any other possible identifications beyond Th III. Similar to HD 143487, the blue triplet component of Th III 6243 Å also appears to be resolved for HD 81588. The Th III 6243 Å line is unfortunately contaminated by a nearby Fe I line, but the position of the extended red wing of the observed feature is consistent with a contribution from Th III. A hint of magnetic splitting can be seen in Th III 6375 Å, albeit not fully resolved. Th III 6461 Å is a blend for all four stars, with the primary contaminant usually being a nearby Ce III line. However, only for CPD-62° 2717 and HD 81588 does the Th III 6461 Å rest wavelength coincide with a local minimum.

Although we consider our search for additional stars with Th III RMSL inconclusive for the time being, it is important to reiterate the point that was made earlier on (see Figures 5 and 6). Namely, whereas the Th III features of CPD-62° 2717 are blatantly present and strong during $\langle B \rangle_{\text{low}}$ phases, they are far less obvious during $\langle B \rangle_{\text{hi}}$ phases. The situation could very well be similar for HD 143487 and HD 81588. For neither star is the amplitude of $\langle B \rangle$ variation nor rotation period known, and thus one cannot rule out the possibility that future observations will take place when severely Th-enhanced portions of their surfaces are in the line-of-sight. We therefore recommend long-term spectroscopic monitoring of HD 143487 and HD 81588 in order to constrain their rotation periods and check for variability similar to that of CPD-62° 2717. Any such observations would ideally extend to $\sim 8400 \text{ Å}$ and thus cover some of the isolated Th III lines that would be expected show resolved magnetic splitting.

Whereas Przybylski’s Star remains uniquely peculiar, the arguably more extreme peculiarities of CPD-62° 2717 firmly place it among

¹ Gaia DR3 orbital solution for HD 143487

the most peculiar stars known. However, it remains to be seen how overabundant thorium actually is on the surface of CPD-62° 2717, by what amplitude that abundance varies as a function of rotation phase, and whether or not any other stars can be shown to have comparable or even higher thorium abundances. Other worthwhile pursuits might include additional spectroscopic and spectropolarimetric monitoring in order to better constrain the rotation period and magnetic field geometry, spectroscopy in other wavelength regimes to search for additional heavy elements, and high-cadence spectroscopy or photometry to check for pulsation. We eagerly anticipate future efforts to address these open questions.

ACKNOWLEDGEMENTS

Funding for the Sloan Digital Sky Survey IV has been provided by the Alfred P. Sloan Foundation, the U.S. Department of Energy Office of Science, and the Participating Institutions. SDSS acknowledges support and resources from the Center for High-Performance Computing at the University of Utah. The SDSS web site is www.sdss.org.

SDSS is managed by the Astrophysical Research Consortium for the Participating Institutions of the SDSS Collaboration including the Brazilian Participation Group, the Carnegie Institution for Science, Carnegie Mellon University, the Chilean Participation Group, the French Participation Group, Harvard-Smithsonian Center for Astrophysics, Instituto de Astrofísica de Canarias, The Johns Hopkins University, Kavli Institute for the Physics and Mathematics of the Universe (IPMU) / University of Tokyo, Lawrence Berkeley National Laboratory, Leibniz Institut für Astrophysik Potsdam (AIP), Max-Planck-Institut für Astronomie (MPIA Heidelberg), Max-Planck-Institut für Astrophysik (MPA Garching), Max-Planck-Institut für Extraterrestrische Physik (MPE), National Astronomical Observatories of China, New Mexico State University, New York University, University of Notre Dame, Observatório Nacional / MCTI, The Ohio State University, Pennsylvania State University, Shanghai Astronomical Observatory, United Kingdom Participation Group, Universidad Nacional Autónoma de México, University of Arizona, University of Colorado Boulder, University of Oxford, University of Portsmouth, University of Utah, University of Virginia, University of Washington, University of Wisconsin, Vanderbilt University, and Yale University.

This work has made use of data from the European Space Agency (ESA) mission Gaia (<https://www.cosmos.esa.int/gaia>), processed by the Gaia Data Processing and Analysis Consortium (DPAC, <https://www.cosmos.esa.int/web/gaia/dpac/consortium>). Funding for the DPAC has been provided by national institutions, in particular the institutions participating in the Gaia Multilateral Agreement.

Based on observations made with ESO telescopes at the La Silla Paranal Observatory under programme IDs 0103.D-0119(A), 0105.D-0193(A), and 0109.D-0226(A).

DATA AVAILABILITY

With the exception of the 2023 April 27 SDSS/APOGEE spectrum of CPD-62° 2717, which is proprietary until the next SDSS data release, all of the [SDSS/APOGEE](#) and [ESO/VLT](#) data used in this paper are publicly available.

REFERENCES

Ahumada R., et al., 2020, [ApJS](#), **249**, 3
Aikman G. C. L., Cowley C. R., Crosswhite H. M., 1979, [ApJ](#), **232**, 812

Aller M. F., Cowley C. R., 1970, [ApJ](#), **162**, L145
Babcock H. W., 1958, [ApJ](#), **128**, 228
Babcock H. W., 1960, [ApJ](#), **132**, 521
Bagnulo S., Landstreet J. D., Lo Curto G., Szeifert T., Wade G. A., 2003, [A&A](#), **403**, 645
Biémont E., Palmeri P., Quinet P., Zhang Z. G., Svanberg S., 2002, [ApJ](#), **567**, 1276
Bolcal C., Kocer D., Koktay T., Guzel T., 1991, [Ap&SS](#), **185**, 237
Caffau E., Sbordone L., Ludwig H. G., Bonifacio P., Steffen M., Behara N. T., 2008, [A&A](#), **483**, 591
Cayrel R., et al., 2001, [Nature](#), **409**, 691
Chojnowski S. D., et al., 2019, [ApJ](#), **873**, L5
Cowley C. R., Greenberg M., 1987, [PASP](#), **99**, 1201
Cowley C. R., Hartoog M. R., 1972, [ApJ](#), **178**, L9
Cowley C. R., Allen M. S., Aikman G. C. L., 1975, [Nature](#), **258**, 311
Cowley C. R., Allen M. S., Aikman G. C. L., 1977, [Astrophys. Lett.](#), **18**, 83
Cowley C. R., Ryabchikova T., Kupka F., Bord D. J., Mathys G., Bidelman W. P., 2000, [MNRAS](#), **317**, 299
Cowley C. R., Bidelman W. P., Hubrig S., Mathys G., Bord D. J., 2004, [A&A](#), **419**, 1087
Dekker H., D’Odorico S., Kaufer A., Delabre B., Kotzlowski H., 2000, in Iye M., Moorwood A. F., eds, *Society of Photo-Optical Instrumentation Engineers (SPIE) Conference Series Vol. 4008, Optical and IR Telescope Instrumentation and Detectors*. pp 534–545, [doi:10.1117/12.395512](https://doi.org/10.1117/12.395512)
Elkin V. G., Mathys G., Kurtz D. W., Hubrig S., Freyhammer L. M., 2010a, [MNRAS](#), **402**, 1883
Elkin V. G., Kurtz D. W., Mathys G., Freyhammer L. M., 2010b, [MNRAS](#), **404**, L104
Elkin V. G., Kurtz D. W., Nitschelm C., 2012, [MNRAS](#), **420**, 2727
Fivet V., Quinet P., Biémont É., Jorissen A., Yushchenko A. V., van Eck S., 2007, [MNRAS](#), **380**, 771
Freyhammer L. M., Elkin V. G., Kurtz D. W., Mathys G., Martinez P., 2008, [MNRAS](#), **389**, 441
Gaia Collaboration et al., 2016, [A&A](#), **595**, A1
Gaia Collaboration et al., 2022, [arXiv e-prints](#), p. [arXiv:2208.00211](https://arxiv.org/abs/2208.00211)
Ghazaryan S., Alecian G., Hakobyan A. A., 2018, [MNRAS](#), **480**, 2953
Giarrusso M., Ceconi M., Cosentino R., Munari M., Ghedina A., Ambrosino F., Boschin W., Leone F., 2022, [MNRAS](#), **514**, 3485
Gunn J. E., et al., 2006, [AJ](#), **131**, 2332
Hill V., et al., 2002, [A&A](#), **387**, 560
Hubrig S., Cowley C. R., Bagnulo S., Mathys G., Ritter A., Wahlgren G. M., 2002, in Tout C. A., van Hamme W., eds, *Astronomical Society of the Pacific Conference Series Vol. 279, Exotic Stars as Challenges to Evolution*. p. 365
Hubrig S., et al., 2005, [A&A](#), **440**, L37
Hubrig S., Järvinen S. P., Madej J., Bychkov V. D., Ilyin I., Schöller M., Bychkova L. V., 2018, [MNRAS](#), **477**, 3791
Jayasinghe T., et al., 2018, [MNRAS](#), **477**, 3145
Kochukhov O., 2008, [A&A](#), **483**, 557
Kochukhov O., Alentiev D., Ryabchikova T., Boyko S., Cunha M., Tsymbal V., Weiss W., 2013, [MNRAS](#), **431**, 2808
Kramida A., Yu. Ralchenko Reader J., and NIST ASD Team 2021, *NIST Atomic Spectra Database (ver. 5.9)*, [Online]. Available: <https://physics.nist.gov/asd> [2022, October 17]. National Institute of Standards and Technology, Gaithersburg, MD.
Kurtz D. W., 1982, [MNRAS](#), **200**, 807
Kurtz D., Wegner G., 1979, [ApJ](#), **232**, 510
Lenz P., Breger M., 2005, [CoAst](#), **146**, 53
Lightcurve Collaboration et al., 2018, *Lightcurve: Kepler and TESS time series analysis in Python*, *Astrophysics Source Code Library (ascl:1812.013)*
Loden L. O., Loden K., Nordstrom B., Sundman A., 1976, [A&AS](#), **23**, 283
Majewski S. R., et al., 2017, [AJ](#), **154**, 94
Mathys G., 2017, [A&A](#), **601**, A14
Mathys G., 2020, in Wade G., Alecian E., Bohlender D., Sigut A., eds, *Vol. 11, Stellar Magnetism: A Workshop in Honour of the Career and Contributions of John D. Landstreet*. pp 35–45 ([arXiv:1912.06107](https://arxiv.org/abs/1912.06107)), [doi:10.48550/arXiv.1912.06107](https://doi.org/10.48550/arXiv.1912.06107)

- Mathys G., Lanz T., 1995, in Sauval A. J., Blomme R., Grevesse N., eds, *Astronomical Society of the Pacific Conference Series Vol. 81, Laboratory and Astronomical High Resolution Spectra*. p. 531
- Mathys G., Hubrig S., Landstreet J. D., Lanz T., Manfroid J., 1997, [A&AS](#), **123**, 353
- Mathys G., Romanyuk I. I., Hubrig S., Kudryavtsev D. O., Schöller M., Semenko E. A., Yakunin I. A., 2019, [A&A](#), **629**, A39
- Mathys G., Kurtz D. W., Holdsworth D. L., 2020, [A&A](#), **639**, A31
- Mathys G., Kurtz D. W., Holdsworth D. L., 2022, [A&A](#), **660**, A70
- Nidever D. L., et al., 2015, [AJ](#), **150**, 173
- Nielsen K. E., Carpenter K. G., Kober G. V., Wahlgren G. M., 2020, [ApJ](#), **899**, 166
- Özdoğan B., et al., 2019, [ApJS](#), **240**, 28
- Pakhomov Y. V., Ryabchikova T. A., Piskunov N. E., 2019, [Astronomy Reports](#), **63**, 1010
- Przybylski A., 1961, [Nature](#), **189**, 739
- Przybylski A., 1963, *Acta Astron.*, **13**, 217
- Przybylski A., 1977, [MNRAS](#), **178**, 71
- Przybylski A., Kennedy P. M., 1963, [PASP](#), **75**, 349
- Redman S. L., Nave G., Sansonetti C. J., 2014, [ApJS](#), **211**, 4
- Rice J. B., 1988, [A&A](#), **199**, 299
- Ricker G. R., et al., 2015, [Journal of Astronomical Telescopes, Instruments, and Systems](#), **1**, 014003
- Ryabchikova T. A., Savanov I. S., Hatzes A. P., Weiss W. W., Handler G., 2000, [A&A](#), **357**, 981
- Ryabchikova T., Ryabtsev A., Kochukhov O., Bagnulo S., 2006, [A&A](#), **456**, 329
- Schatz H., Toenjes R., Pfeiffer B., Beers T. C., Cowan J. J., Hill V., Kratz K.-L., 2002, [ApJ](#), **579**, 626
- Shulyak D., Ryabchikova T., Kildiyarova R., Kochukhov O., 2010, [A&A](#), **520**, A88
- Wilson J. C., et al., 2019, [PASP](#), **131**, 055001
- Wolff S. C., Hagen W., 1976, [PASP](#), **88**, 119
- Zasowski G., et al., 2013, [AJ](#), **146**, 81

This paper has been typeset from a \LaTeX file prepared by the author.